

Evodiamine suppresses the progression of non-small cell lung carcinoma via endoplasmic reticulum stress-mediated apoptosis pathway *in vivo* and *in vitro*

International Journal of
Immunopathology and Pharmacology
Volume 36: 1–17
© The Author(s) 2022
Article reuse guidelines:
sagepub.com/journals-permissions
DOI: 10.1177/03946320221086079
journals.sagepub.com/home/iji
SAGE

Yuting Li^{1,2,3}, Yuming Wang¹, Xiaoqun Wang^{2,3}, Lulu Jin¹, Lu Yang¹, Jinli Zhu^{2,3}, Hongwu Wang¹, Fang Zheng¹, Huantian Cui⁴ , Xiaojiang Li^{2,3} and Yingjie Jia^{2,3}

Abstract

Background: Evodiamine (EVO) is one of the major components isolated from *Evodia rutaecarpa* (Juss.). Recent studies have shown that EVO has an anti-cancer effect. However, the pharmacological mechanism by which EVO impacts cancer is still poorly understood.

Objectives: This study focused on asking the anti-cancer effect of EVO in human non-small cell lung carcinoma (NSCLC), and in particular to investigate whether EVO acts via modulating the endoplasmic reticulum stress (ERS)-mediated apoptosis pathway.

Materials and Methods: A Lewis lung carcinoma (LLC) tumor-bearing mouse model was treated with low-dose EVO (5 mg/kg) and high-dose EVO (10 mg/kg) intraperitoneally for 14 d. The effects of EVO on tumor growth, apoptosis, and ERS were assessed. In addition, NSCLC A549 and LLC cells were treated with EVO *in vitro*. The effects of EVO on cell proliferation, apoptosis, and ERS were investigated. Finally, 4-phenylbutyric acid (4-PBA), an ERS inhibitor, was used to validate whether EVO induced apoptosis of NSCLC cells by modulating ERS.

Results: EVO treatment significantly inhibited tumor growth in LLC tumor-bearing mice. H&E staining indicated that EVO treatment reduced the number of tumor cells and the nucleo-plasmic ratio. Immunostaining showed that EVO treatment significantly decreased the expression of Ki-67. TUNEL staining revealed that EVO induced apoptosis in the tumor. Likewise, EVO treatment up-regulated the expression of apoptosis-related genes and proteins and increased activation of the ERS pathway in the tumor. Additionally, EVO inhibited cell proliferation and increased cell apoptotic rates in A549 and LLC cells. EVO also increased the expression levels of genes and proteins associated with ERS-mediated apoptosis pathway *in vitro*. The effects of EVO on apoptosis were abolished by 4-PBA treatment.

¹First Teaching Hospital of Tianjin University of Traditional Chinese Medicine, Tianjin, China

²National Clinical Research Center for Chinese Medicine Acupuncture and Moxibustion, Tianjin, China

³Tianjin University of Traditional Chinese Medicine, Tianjin, China

⁴Shandong Provincial Key Laboratory of Animal Cell and Developmental Biology, School of Life Sciences, Shandong University, Qingdao, China.

Yuting Li, Yuming Wang, and Xiaoqun Wang are co-first authors on this work.

Corresponding authors:

Huantian Cui, Shandong Provincial Key Laboratory of Animal Cell and Developmental Biology, School of Life Sciences, Shandong University, Qingdao, China.

Email: 1762316411@qq.com

Xiaojiang Li, First Teaching Hospital of Tianjin University of Traditional Chinese Medicine, Tianjin, China.

Email: Li_xj2020@126.com

Yingjie Jia, First Teaching Hospital of Tianjin University of Traditional Chinese Medicine, Tianjin, China.

Email: jiayingjie1616@sina.com



Creative Commons Non Commercial CC BY-NC: This article is distributed under the terms of the Creative Commons Attribution-NonCommercial 4.0 License (<https://creativecommons.org/licenses/by-nc/4.0/>) which permits non-commercial use, reproduction and distribution of the work without further permission provided the original work is attributed as specified on the SAGE and Open Access pages (<https://us.sagepub.com/en-us/nam/open-access-at-sage>).

Conclusions: Our study demonstrated that EVO suppresses the progression of NSCLC by modulating the ERS-mediated apoptosis pathway.

Keywords

Evodiamine, non-small cell lung carcinoma, lewis lung carcinoma cells, A549 cells, endoplasmic reticulum stress, apoptosis

Introduction

Currently, lung cancer carries the highest mortality rate of any malignant tumor. In 2020, there were more than 2.21 million new cases of lung cancer and 1.80 million deaths caused by lung cancer.¹ Non-small cell lung carcinoma (NSCLC) accounts for about 80% of all lung cancers.² Despite advances in surgical resection, radiotherapy, chemotherapy, and other medical treatments, NSCLC patients face a low overall survival rate (approximately 20%) and dismal prognosis.^{3,4} It is of special urgency to development new therapeutics for NSCLC.

In recent years, there has been increasing attention on the important role of endoplasmic reticulum stress (ERS) in the homeostasis of cancer cells.^{5,6} The endoplasmic reticulum (ER) is an important organelle whose functions include folding and trafficking of proteins, maintaining calcium homeostasis, initiating lipid synthesis, and participating in a number of crucial cellular functions.⁷ ERS is caused by an overload of misfolded or unfolded proteins in the ER. Under physiological conditions, a signaling network called the unfolded protein response (UPR) is triggered to enhance the folding capacity of ER and reduce the folding load, resulting in the re-establishment of cell homeostasis.⁸ Prolonged and excessive ERS is considered a major trigger of apoptosis signaling pathways.⁹ Therefore, ERS is a potential target for exploring novel drugs which interfere with specific signaling pathways to induce cancer cell apoptosis.¹⁰ For instance, hispidulin activates ERS-mediated apoptosis in hepatocellular carcinoma cells via regulating AMPK/mTOR pathway.¹¹ Similarly, curcumin effectively enhances tumor cell apoptosis in NSCLC H460 cells through activating ERS.¹²

Evodiamine (EVO) is one of the major components isolated from *Evodia rutaecarpa* (Juss.). EVO has been demonstrated with various biological effects, including anti-inflammatory,¹³ antinociceptive,¹⁴ anti-obesity,¹⁵ and vasodilatory effects.¹⁶ In recent years, growing evidence demonstrates that EVO has anti-cancer potential both in vitro and in vivo by inhibiting tumor proliferation, invasion and metastasis, and inducing apoptosis of multiple tumor cells.¹⁷⁻²⁰ Previous studies have also demonstrated that EVO could induce apoptosis of human small-cell lung cancer cells through modulating ER-related pathway.²¹ However, the anti-tumor effect of

EVO in vivo have not been studied, and the detailed mechanism by which EVO modulating ERS to induce tumor apoptosis is unclear.

In the current study, an LLC tumor-bearing mouse model was established and treated with low-dose EVO (5 mg/kg) and high-dose EVO (10 mg/kg) intraperitoneally for 14 d, whereupon the effects of EVO on tumor growth, apoptosis and ERS were assessed. Additionally, NSCLC A549 and LLC cells were treated with EVO in vitro. The effects of EVO on cell proliferation, apoptosis and ERS were investigated. Finally, 4-phenylbutyric acid (4-PBA), an ERS inhibitor, was used to validate whether EVO induced the apoptosis of NSCLC cells by modulating ERS. Our studies could open avenues to understand the anti-tumor effects and mechanisms of EVO and could provide scientific evidence of clinic use of EVO on tumor treatment.

Materials and methods

Reagents

EVO, with a purity >98%, was purchased from Pharmagenesis Inc. (Beijing, China) (Figure 1(a)). Cisplatin (CDDP), with a purity >98.5%, was obtained from Dalian Meilun Biotechnology Co., Ltd. (Liaoning, China). 4-PBA (HY-15,654), with a purity of 99.80%, was purchased from MedChemExpress Co., Ltd. (Shanghai, China) (Figure 1(b)). Rabbit polyclonal antibodies against glucose-regulated protein 78 (GRP78) (bs-1219R), cysteinyl aspartate specific proteinase (caspase) –12 (bs-1105R), and inositol-requiring enzyme 1 (IRE1) (bs-16,696R) were obtained from Bioss Bioscience Co., Ltd. (Beijing, China). Apoptotic signal-regulating kinase 1 (ASK1) (67,072-1-Ig), mouse monoclonal antibody, and rabbit anti- β -actin (20,536-1-AP) were purchased from Proteintech, Inc. (Wuhan, China). Rabbit monoclonal antibodies against B-cell lymphoma-2 (Bcl-2) (ab59348), Bcl-2 associated X protein (Bax) (ab32503), caspase-9 (ab184786), tumor necrosis factor (TNF) receptor associated factor 2 (TRAF2) (ab126758), caspase-3 (ab13847), Ki-67 (ab15580), and HRP-conjugate goat anti-rabbit IgG (ab205718) were obtained from Abcam, Inc. (Shanghai, China). Rabbit c-JUN amino-terminal kinase (JNK) (#9252) and p-JNK (#4668) antibodies were obtained from Cell Signaling Technology, Inc. (Shanghai, China). A terminal deoxynucleotidyl transferase-mediated dUTP nick

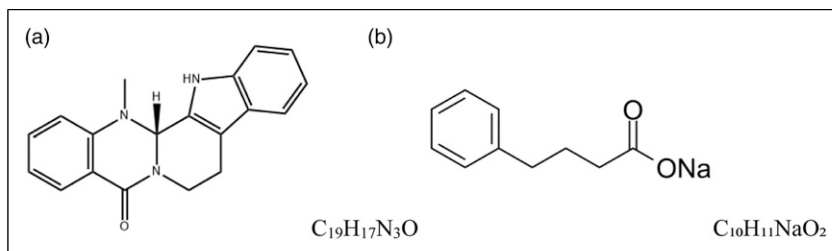


Figure 1. Chemical structures. **(a)** Chemical structure of evodiamine (EVO). **(b)** Chemical structure of sodium 4-phenylbutyrate (4-PBA).

end-labeling (TUNEL) test kit was purchased from Nanjing Jiancheng Biological Engineering Institute (Nanjing, China). A total RNA extraction kit, first-stand cDNA reverse transcription kit, polymerase chain reaction kit and primers were obtained from TianGen Biotechnology Co., Ltd. (Beijing, China). Sodium dodecyl sulfate-polyacrylamide gel electrophoresis (SDS-PAGE), Phosphate-Buffered Saline (PBS), PVDF membranes, BCA protein assay kit, penicillin/streptomycin (PS), dimethyl sulfoxide (DMSO), and 0.25% Trypsin-0.53 mM EDTA were purchased from Solarbio Biotechnology Co., Ltd. (Beijing, China). Fetal bovine serum (FBS) and Roswell Park Memorial Institute (RPMI) medium were purchased from Hyclone Bioscience Co., Ltd. (Beijing, China). Dulbecco's Modified Eagle Medium (DMEM) was purchased from Gibco Biotechnology Co., Ltd. (Beijing, China). A [3-(4,5-dimethylthiazol-2-yl)2,5-diphenyltetrazolium bromide] (MTT) kit was obtained from BD Biosciences (Franklin Lakes, NJ, USA). An annexin V-fluorescein isothiocyanate (FITC)/propidium iodide (PI) apoptosis detection kit was purchased from KeyGEN BioTHCHB Co., Ltd. (Jiangsu, China).

Cell culture

LLC and human NSCLC A549 cell lines were obtained from Shanghai Institutes for Biological Sciences (Shanghai, China). The A549 cell line was cultured in RPMI-1640 medium added with 10% FBS, PS (100 U/mL and 100 μ g/mL, respectively), while the LLC cell line was grown in DMEM supplemented with 10% FBS, PS (100 U/mL and 100 μ g/mL, respectively). The cells were maintained in a 37°C humidified incubator containing 5% CO₂. The medium was replaced every 24 h. After incubation for 48 h, these cell lines were digested with 0.25% Trypsin-0.53 mM EDTA and passaged, selecting the cells exhibiting logarithmic growth for further experimentation.

Cell viability assay

The cells with logarithmic growth were seeded into 96-well plates (10⁴ cells/well) and cultured up to 24 h until adherence. Subsequently, EVO was dissolved in DMSO

(10 mM) and the concentration of DMSO in the cell culture medium was <0.1%. Then, A549 and LLC cells were treated with different concentrations of EVO (0, 1, 2, 5, 10, 20, 50, and 100 μ M) and incubated for either 24 h or 48 h. After that, 20 μ L of MTT solution (5 mg/mL) was supplemented to cells and they were further incubated at 37°C for 4 h. After incubation, the medium was carefully removed and cells were resolved by 200 μ L DMSO. The optical density was measured at 490 nm by a microplate reader (Varioskan Flash, Thermo) to calculate the half maximal inhibitory concentration (IC₅₀) values. The percentage of cell viability was computed as follows: cell viability (%) = A₄₉₀ (EVO)/A₄₉₀ (control) × 100%.

Animals and treatment

A total of 40 male C57BL/6 mice, 5 weeks old and weighing 18–22 g, were obtained from Huaafukang Animal Co., Ltd. (Beijing, China). The Animal Experiment Ethics Committee of Tianjin University of Traditional Chinese Medicine approved all reported animal experiments (Registration No.: SYXK2019-0108, date of approval: 2019-07-13). All mice were housed in a controlled environment (12 h light/dark cycle, temperature of 22 ± 2°C and humidity of 45 ± 10%). After acclimatization, LLC cells (5 × 10⁵, viability ≥95%) were subcutaneously injected into the right forelimb of mice to induce the LLC tumor-bearing mouse model.²² When the tumor size reached 100 mm³, the mice were randomly divided into 4 groups (n = 10 for each group): model group (0.2 mL normal saline, intraperitoneal (i.p.) injection, once a day), positive control group (6 mg/kg CDDP, i.p. injection, once every 2 days), EVO low-dose group (5 mg/kg EVO, i.p. injection, once a day), and EVO high-dose group (10 mg/kg EVO, i.p. injection, once a day).^{23,24} The tumor size was measured using calipers every 2 days and the tumor volume was evaluated using the following formula: volume (mm³) = length (mm) × width (mm) × width (mm)/2²⁵. All intervention treatments lasted for 14 days and mice were supplied a standard rodent diet and water ad libitum during experimental periods.

At the end of the 14 d EVO treatment, all surviving mice were euthanized by cervical dislocation and the mouse

tumor tissue was removed immediately and weighed. Tumor inhibition rate was evaluated according to the following formula: tumor growth inhibition rate (%) = (1 -

mean tumor weight of the treatment group/mean tumor weight of the non-treatment group) × 100%.

Table 1. Primer sequences used for the mouse target genes.

Genes	Primer sequence (5'-3')
<i>Actb</i>	Forward: AGCCATGTACGTAGCCATCC Reverse: CTCTCAGCTGTGGTGGTGAA
<i>Grp78</i>	Forward: AGTGGTGGCCACTAATGGAG Reverse: CAATCCTTGCTTGATGCTGA
<i>Irel</i>	Forward: ACTGTGGATCCAGGAAGTGG Reverse: GTCTTGGTAGCTGGAGGCAG
<i>Traf2</i>	Forward: GCCAGATTTGGAGCAGAAG Reverse: CCAGCTGTTGCACCTTGTTA
<i>Map3k5</i>	Forward: GCCAGAGCTAAGTCCTGTGG Reverse: TGGGCCAGAGATTCCATTAG
<i>Mapk9</i>	Forward: GGTGAATATTTGGATGAAGCC Reverse: CCTTGAGCTCCTGAGCCTAT
<i>Bax</i>	Forward: TGCAGAGGATGATTGCTGAC Reverse: GATCAGCTCGGGCACTTTAG
<i>Bcl2</i>	Forward: CTGAGTACCTGAACCGGCAT Reverse: CTCACCTGTGGCCCAGGTAT

Table 2. Primer sequences used for the human target genes.

Genes	Primer sequence (5'-3')
<i>Actb</i>	Forward: GGACTTCGAGCAAGAGATGG Reverse: AGCACTGTGTTGGCGTACAG
<i>Grp78</i>	Forward: TAGCGTATGGTGTCTGCTGTC Reverse: TTTGTGAGGGGTCTTTCACC
<i>Irel</i>	Forward: CGGCCTTTGCAGATAGTCTC Reverse: ACGTCCCCAGATTCACCTGTC
<i>Traf2</i>	Forward: CGGCCACTTTTGAGAACATT Reverse: CCAAGACCTTCTGCTCCAAG
<i>Map3k5</i>	Forward: TCCAAATGGGGTCCATTAAA Reverse: TTATGCCAGCAAGCCTCTTT
<i>Mapk9</i>	Forward: TTGGAACACCATGTCCTGAA Reverse: ATGTACGGGTGTTGGAGAGC
<i>Bax</i>	Forward: TTTGCTTCAGGGTTTCATCC Reverse: CAGTTGAAGTTGCCGTCAGA
<i>Bcl2</i>	Forward: GAGGATTGTGGCCTTCTTTG Reverse: ACAGTTCCACAAAGGCATCC

Table 3. Tumor weight and tumor growth inhibition rate.

Group	Tumor weight (g)	Tumor growth inhibition rate (%)
Model	1.89 ± 0.42	-
Positive control	1.11 ± 0.30**	41.45 ± 9.99
EVO low-dose	1.50 ± 0.34**	20.55 ± 8.36###
EVO high-dose	1.21 ± 0.37**	36.55 ± 10.65

Model, positive control, EVO low-dose and EVO high-dose (n = 10 per group) groups. Data are presented as mean ± SD. *: p < 0.05 compared with model group; **: p < 0.01 compared with model group; #: p < 0.05 compared with positive control group; ###: p < 0.01 compared with positive control group.

H&E staining and immunohistochemistry

After 14 d of EVO treatment, H&E staining was conducted to facilitate histological evaluation as described previously.²⁶ Specifically, tumors were fixed in 4% paraformaldehyde, embedded in paraffin and cut into 5-µm-thick sections. Then the sections were stained with hematoxylin and eosin (H&E).

The expression of Ki-67 in tumor tissue was detected by immunohistochemistry. After being deparaffinized and rehydrated, embedded samples were processed with trypsin for 10 min or heat for 25 min and subsequently incubated with Ki-67 primary antibody overnight. After incubation of primary antibody, secondary antibody was added and the sections were incubated for 30 min. Stain was developed using peroxidase 3,30-diaminobenzidine (DAB) substrate and counterstained with hematoxylin. The integrated optical density (IOD) and mean optical density (MOD) were quantified using Image-pro Plus 6.0 software. MOD=IOD sum/area sum.

Tunel analysis

Tissue paraffin sections were prepared, dewaxed in xylene, and hydrated in ethanol. Then the TUNEL reaction solution was added according to the TUNEL kit instructions, following which DAB solution as the chromogenic substrate was added to each section. Finally, apoptosis was observed under fluorescence microscope after being rinsed with PBS.²⁷ The ratio of apoptotic cells to the total cells was quantified by Image-pro Plus 6.0 software based on IOD.

Western blot analysis

In brief, protein samples, which were extracted from tumor tissue, A549 or LLC cells, were standardized using a BCA protein assay kit, loaded onto 8–12% SDS-PAGE, transferred to a PVDF membrane, and blocked with Tween-Tris-buffered saline (TBST) solution supplemented with 5% BSA. Subsequently, the membrane

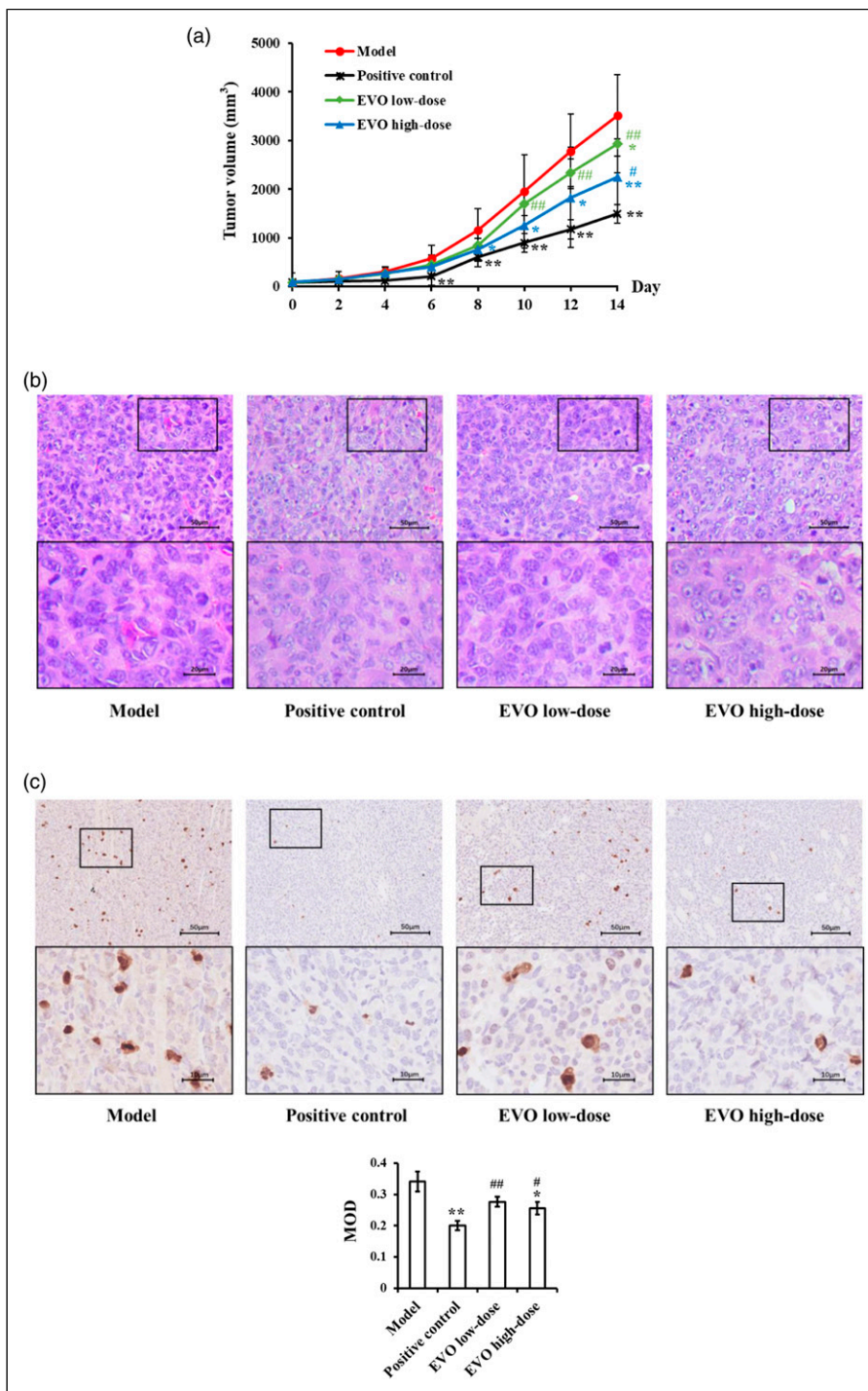


Figure 2. The anti-tumor effect of EVO on LLC tumor-bearing mice. **(a)** EVO showed significant inhibition of tumor volume. **(b)** Results of H&E staining indicated that EVO treatment reduced the number of tumor cells and nucleo-plasmic ratio ($\times 200$ and $\times 400$ magnification) compared to the model group. **(c)** Immunostaining indicated that EVO treatment markedly decreased the expression of Ki-67 ($\times 200$ and $\times 800$ magnification). Data are presented as the mean \pm SD. *: $p < 0.05$ compared with model group; **: $p < 0.01$ compared with model group; #: $p < 0.05$ compared with positive control group; ###: $p < 0.01$ compared with positive control group.

was incubated with primary antibody (rabbit anti-IRE1 1:2000, rabbit anti-GRP78 1:2000, rabbit anti-TRAF2 1:1000, mouse anti-ASK1 1:6000, rabbit anti-JNK 1:1000, rabbit anti-p-JNK 1:1000, rabbit anti-Bax 1:8000, rabbit anti-Bcl-2 1:1000, rabbit anti-caspase-12 1:2000, rabbit anti-caspase-9 1:1000, rabbit anti-caspase-3 1:500, and rabbit anti- β -actin 1:5000) at 4°C overnight. The next day, after being washed with TBST, these membranes were incubated with secondary antibody (HRP-conjugate goat anti-rabbit IgG 1:10,000) for 2 h at room temperature, followed by enhanced chemiluminescence. Blotting was visualized using chemiluminescence (ChemiScope 3000mini, Clinx Science Instruments Co., Ltd., Shanghai, China) following the manufacturer's instructions. β -actin was selected as an internal control to compare protein levels. The intensity of the bands was determined based on Image J software.

RNA isolation and real-time reverse transcription quantitative polymerase chain reaction

Total RNA was extracted from tumor tissue, A549 or LLC cells using an RNA extraction kit following the manufacturer's protocol. The purity of RNA was measured by the ratio of optical densities at 260 and 280 nm. 1 μ g of total RNA was used to synthesize first-strand cDNA. The cycling programs

were as follows: 95°C for 15 min, 40 cycles of 95°C for 10 s. The expression levels of *Grp78*, *Ire1*, *Traf2*, *mitogen-activated protein kinase kinase kinase 5* (*Map3k5*, also called *ASK1*), *mitogen-activated protein kinase 9* (*Mapk9*, also named *JNK*), *Bax*, and *Bcl2* in tumor tissue, A549 or LLC cells were measured using Quantitative RT-PCR (qPCR) as previously reported.²⁸ These samples were examined in triplicate by a BIORAd iQ5 detection system. *Actb* was used as an internal control. Quantification was carried out based on the $2^{-\Delta\Delta CT}$ method.²⁹ The primers for target genes were designed using the NCBI GeneBank database and sequences of primers are listed in Tables 1 and 2.

Flow cytometric analysis

The cell apoptosis was quantified using Annexin V-FITC/PI detection kit. LLC and A549 cells were seeded in 6-well plates at 37°C for 24 h. Then, cells were treated with trypsin, washed with PBS, centrifuged at 2000 rpm for 5 min, and resuspended in 500 μ L binding buffer. Subsequently, cells were incubated with 5 μ L PI working solution and 5 μ L Annexin V-FITC at room temperature and dark for 15 min. Next, these samples were detected by a FACScan flow cytometer (BD Biosciences, Franklin Lakes, NJ, USA) and analyzed using FlowJo software.

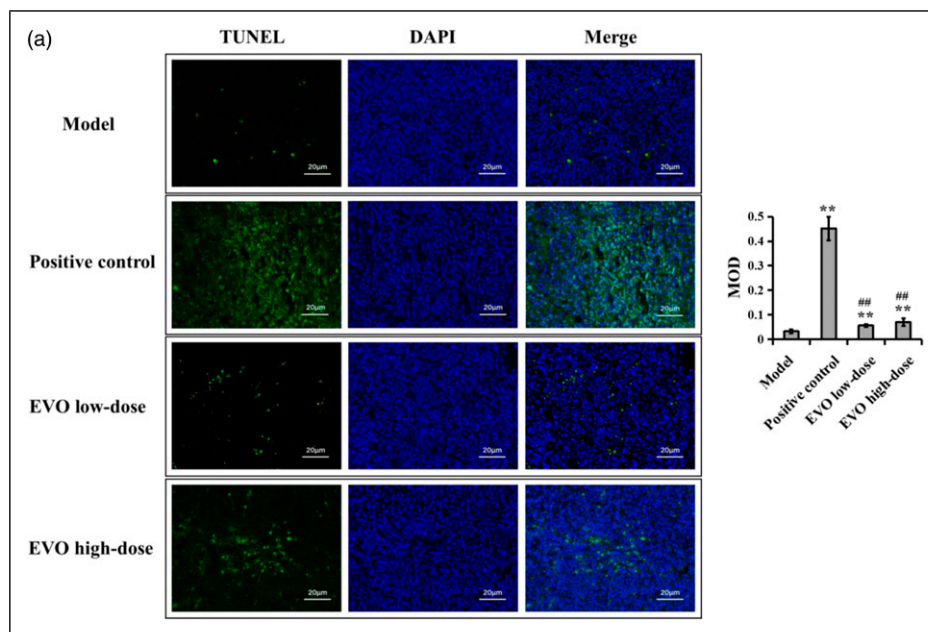


Figure 3. EVO triggered apoptosis in LLC tumor-bearing mice in vivo. (a) TUNEL staining showed that EVO and CDDP treatment increased the number of apoptotic cells in the tumor compared to the model group. (b) EVO up-regulated the protein expressions of TRAF2, ASK1, JNK, p-JNK, caspase-12, -9, -3, and Bax and down-regulated Bcl-2 expression in tumor tissue. β -actin was used to confirm equal protein loading. (c) EVO increased the mRNA levels of *Traf2*, *Map3k5*, *Mapk9*, *Bax*, and decreased *Bcl2* level in tumor tissue. Data are expressed as means \pm SD. *: $p < 0.05$ compared with model group; **: $p < 0.01$ compared with model group; ###: $p < 0.01$ compared with positive control group. Abbreviations: c-c12/t-c12: cleaved caspase-12/total caspase-12; c-c9/t-c9: cleaved caspase-9/total caspase-9; c-c3/t-c3: cleaved caspase-3/total caspase-3.

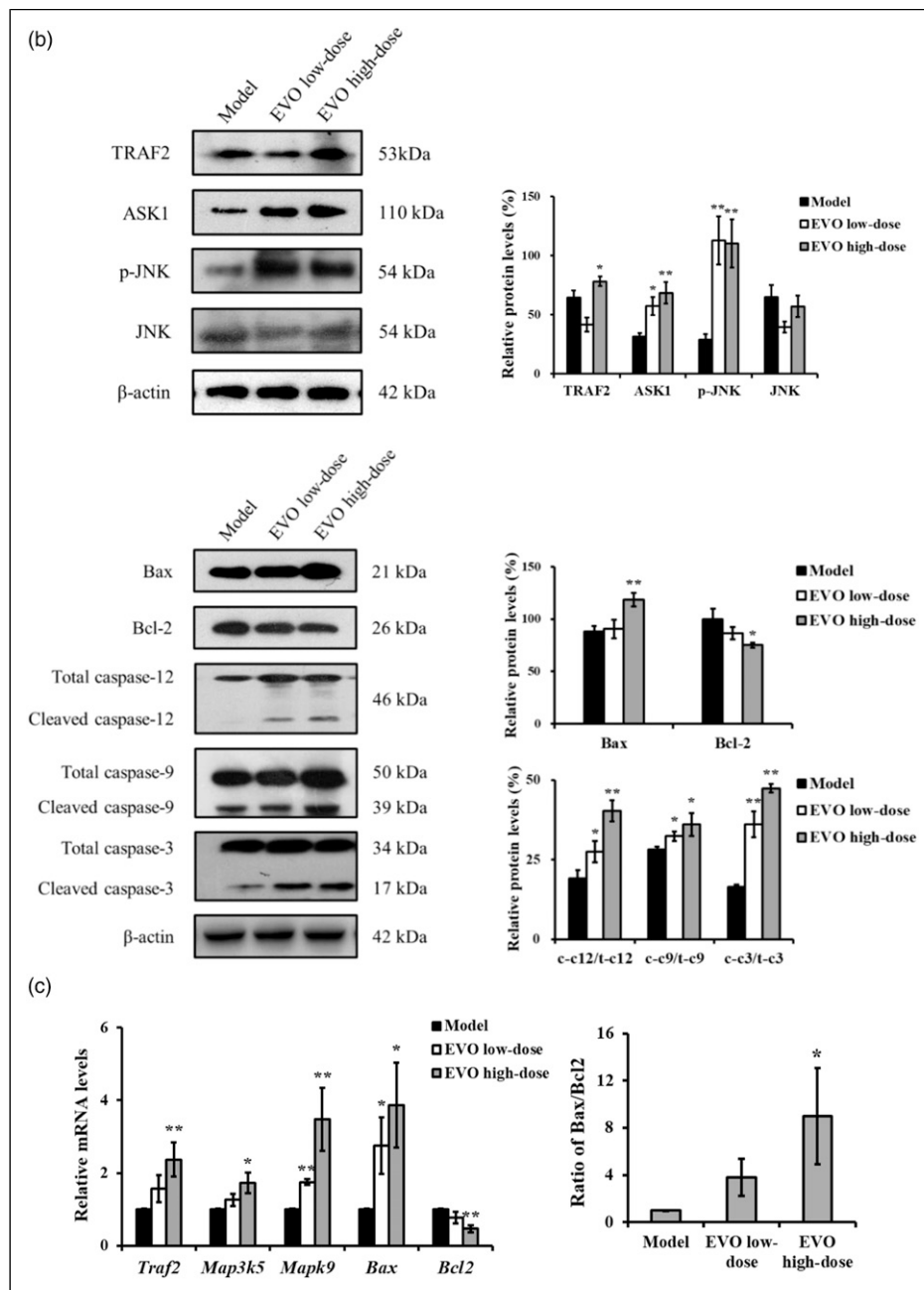


Figure 3. Continued.

Statistics

The independent experimental data were analyzed using mean \pm standard deviation (mean \pm SD). Analysis of variance (ANOVA) was used to test the statistical differences between the experimental groups, followed by Dunnett's test. Statistical significance was set at a p-value $<$ 0.05, and analyses were conducted using SPSS version 20.0. Curve-fitting was performed using the graphical package GraphPad Prism5.

Results

Anti-tumor effect of Evodiamine (EVO) on lewis lung carcinoma tumor-bearing mice

Following the 14 d EVO treatment, tumor weight was significantly decreased in the positive control, EVO low-dose and EVO high-dose groups compared with that in model group (Table 3). The tumor growth inhibition rates in positive control, EVO low-dose and EVO high-dose

groups were $41.45 \pm 9.99\%$, $20.55 \pm 8.36\%$, and $36.55 \pm 10.65\%$, respectively (Table 3). The tumor weight and tumor growth inhibition rate were visibly higher in the EVO low-dose group compared with the positive control group, but there were no significant differences between the EVO high-dose group and positive control group (Table 3). Additionally, the growth of tumors in the model group was rapid, whereas the tumor growth with low-dose or high-dose EVO treatment was delayed. However, the tumor volume was higher in low-dose and high-dose EVO groups compared with that in positive group. In sum, compared to the model group both low-dose and high-dose EVO showed significant inhibition of tumor volume over time (Figure 2(a)).

H&E staining of tumor tissues indicated that the tumor cells in the model group were evenly and closely distributed, with large and hyperchromatic cell nuclei, whereas both EVO and CDDP treatment resulted in loose cell arrangement, cytoplasmic contraction, reduced nucleo-plasmic ratio, and relatively shallow tumor cell staining (Figure 2(b)). Moreover, immunostaining indicated that the cell proliferative marker (Ki-67) was positively expressed in the model group, whereas CDDP and high-dose EVO treatment markedly decreased the expression of Ki-67 in tumors. However, the expression of Ki-67 was obviously higher in the EVO low-dose and EVO high-dose groups compared with positive control group (Figure 2(c)).

Effect of EVO on apoptosis in lewis lung carcinoma tumor-bearing mice in vivo

The numbers of TUNEL-positive cells were increased in positive control, EVO low-dose, and EVO high-dose groups compared with the model group, and the number of apoptotic cells was lower in EVO low-dose and EVO high-dose groups compared with the positive control group (Figure 3(a)). Furthermore, compared with the model group, high-dose EVO treatment increased activation of TRAF2, ASK1, p-JNK, caspase-12, -9, -3, and Bax, and decreased the expression of Bcl-2, which were closely related to cell apoptosis. Although its effects were not as wide-ranging as the high-dose group, a low dose of EVO significantly elevated expression levels of ASK1, p-JNK, caspase-12, -9, and -3 (Figure 3(b)). Similarly, high-dose EVO affected all measured mRNA levels, increasing *Traf2*, *Map3k5*, *Mapk9*, and *Bax*, and decreasing the mRNA level of *Bcl2*, and also significantly elevated the ratio of Bax/Bcl-2. Low-dose EVO had a similar but more limited effect, significantly increasing mRNA levels in *Mapk9* and *Bax* (Figure 3(c)).

Effect of EVO on ERS in lewis lung carcinoma tumor-bearing mice in vivo

To examine the effect of EVO on the ERS response, we measured the expression of ERS-associated proteins by

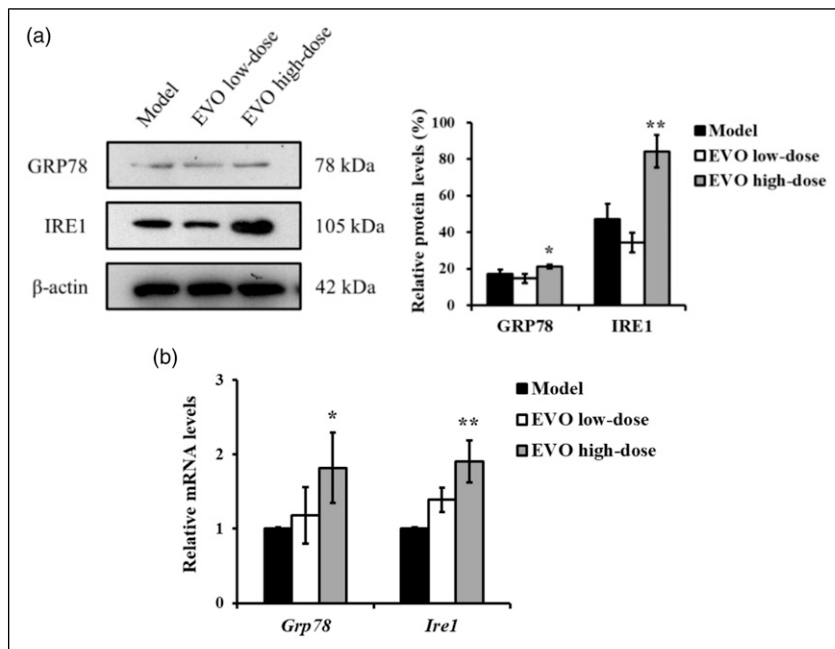


Figure 4. EVO promoted ERS in LLC tumor-bearing mice in vivo. (a) EVO increased the protein expressions of GRP78 and IRE1 in tumor tissue. β -actin was used to confirm equal protein loading. (b) EVO up-regulated the mRNA expressions of *Grp78* and *Ire1* in the tumor. Data are expressed as means \pm SD. *: $p < 0.05$ compared with model group; **: $p < 0.01$ compared with model group.

western blot and qPCR. As shown in Figure 4(a), the expression levels of GRP78 and IRE1 were higher in the EVO high-dose group compared with the model group (Figure 4(a)). In addition, the mRNA levels of *Grp78*, and *Ire1* were significantly increased following high-dose EVO treatment (Figure 4(b)).

Effects of EVO on cell proliferation and apoptosis in A549 and lewis lung carcinoma cells

The effect of EVO on cell viability was evaluated in A549 and LLC cells with different concentrations (0, 1, 2, 5, 10, 20, 50, and 100 μM) and time points (24 and 48 h) by MTT assay. The results showed dose- and time-dependent effects of EVO on the viability of LLC and A549 cells (Figure 5(a) and (b)). Notably, IC_{50} values were determined using

GraphPad Prism (GraphPad Software Inc. San Diego, CA, U.S.A.), and the IC_{50} value of A549 cells was 22.44 μM after 24 h of EVO treatment and the IC_{50} value of LLC cells was 6.86 μM following 48 h of EVO intervention. Specific concentrations of EVO were selected for further in vitro studies based on IC_{50} and $1/2 \text{IC}_{50}$ values (22.44 μM and 11.22 μM EVO for 24 h in A549 cells; 6.86 μM and 3.43 μM EVO for 48 h in LLC cells).

Flow cytometry, western blot and qPCR were used to determine whether EVO could induce apoptosis in A549 and LLC cells. EVO was added to A549 or LLC cells and the apoptosis rates were then measured by flow cytometry. As shown in Figure 5(c), the apoptosis rates in both A549 and LLC cells were significantly increased following EVO treatment, with higher apoptosis rates associated with higher levels of EVO (Figure 5(c)). These results suggest

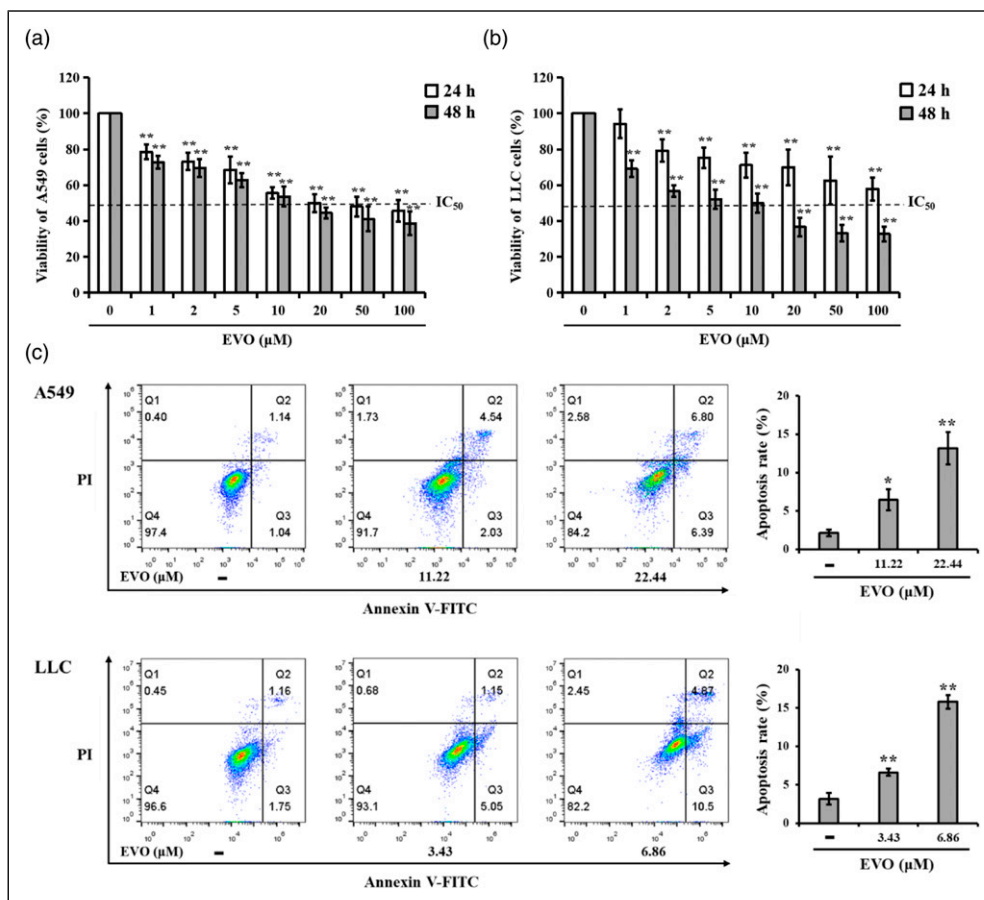


Figure 5. EVO inhibited cell viability and activated apoptosis in A549 and LLC cells. (a, b) EVO inhibited the viability of A549 (a) and LLC (b) cells in a dose- and time-dependent manner. Cell viability was investigated using MTT assay. (c) EVO-induced apoptosis was observed by flow cytometry and apoptotic rate was quantified. (d) EVO increased the expression levels of TRAF2, ASK1, p-JNK, caspase-12, -9, -3, and Bax, and decreased the expression level of Bcl-2 in A549 and LLC cells. β -actin was used to confirm equal protein loading. (e, f) qPCR revealed EVO-induced increases in the mRNA levels of *Traf2*, *Map3k5*, *Mapk9*, *Bax*, and a decrease in the mRNA level of *Bcl2* in A549 and LLC cells. Data are expressed as means \pm SD. *: $p < 0.05$ compared with EVO (–) group; **: $p < 0.01$ compared with EVO (–) group. Abbreviations: c-c12/t-c12: cleaved caspase-12/total caspase-12; c-c9/t-c9: cleaved caspase-9/total caspase-9; c-c3/t-c3: cleaved caspase-3/total caspase-3.

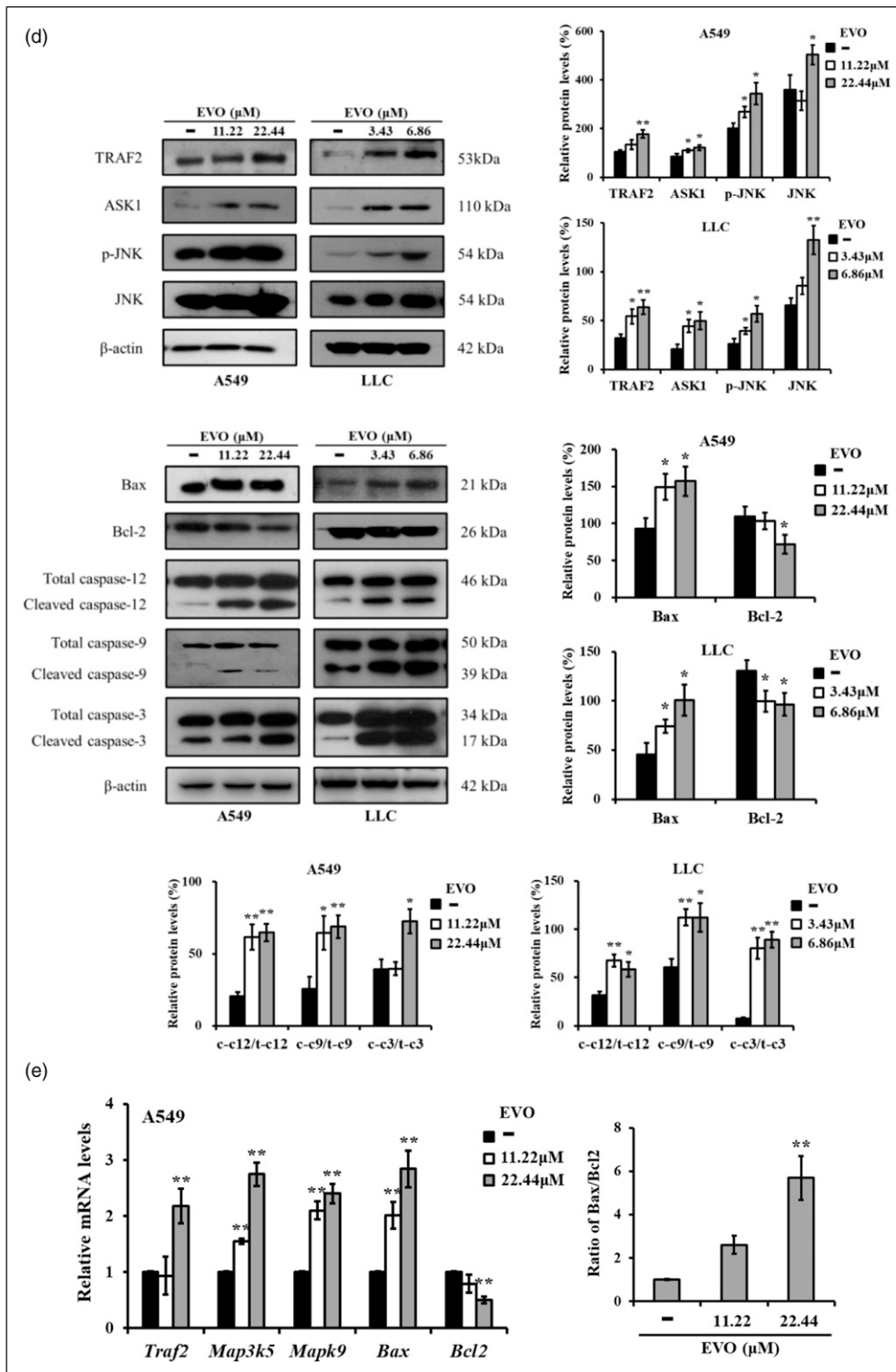


Figure 5. Continued.

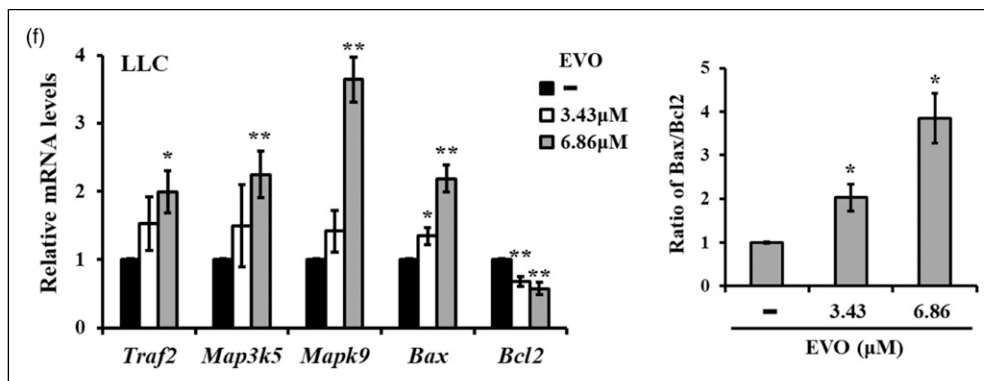


Figure 5. Continued.

that targeted EVO treatment at specific concentrations can increase apoptosis rates in NSCLC. Higher expression levels for TRAF2, ASK1, p-JNK, caspase-12, -9, -3, and Bax and lower expression levels for Bcl-2 were observed following EVO treatment, in a dose-dependent manner (Figure 5(d)). After 24 h of adding 11.22 μM and 22.44 μM EVO to A549 cells and 48 h of 3.43 μM and 6.86 μM EVO treatment to LLC cells, mRNA levels of *Traf2*, *Map3k5*, *Mapk9*, and *Bax* were significantly increased whereas *Bcl-2* mRNA level was significantly decreased compared with the EVO (–) group (Figure 5(e) and (f)). Finally, the ratio of Bax/Bcl2 was elevated after treatment with EVO (Figure 5(e) and (f)).

Effects of EVO on ERS and apoptosis in A549 and lewis lung carcinoma cells in vitro

Levels of ERS-related proteins were examined in A549 and LLC cells. Results indicated that protein levels of GRP78 and IRE1 were visibly higher in both A549 and LLC cells after EVO treatment (Figure 6(a)). Likewise, EVO intervention up-regulated mRNA levels of *Grp78*, and *Irel* in A549 and LLC cells (Figure 6(b) and (c)).

According to previous studies, ERS can be significantly inhibited by 100 μM 4-PBA, an ERS inhibitor, for 24 h.³⁰ To further explore the relationship between ERS and EVO-induced apoptosis, the A549 and LLC cells were pretreated with 4-PBA (100 μM) for 24 h. Specific concentrations and intervention times for EVO were selected for further studies based on IC_{50} values (22.44 μM EVO to A549 cells for 24 h; 6.86 μM EVO to LLC cells for 48 h). Compared with the EVO only treatment group, the apoptotic rate was lower in the 4-PBA pretreatment group, but the apoptotic rate was not significantly increased following treatment with 4-PBA and EVO (Figure 6(d)).

Previous studies have demonstrated that TRAF2 can be recruited by IRE1 cytosolic kinase and induce the formation of the IRE1/TRAF2/ASK1 complex, subsequently activate JNK pathway.³¹ As shown in Figure 6(e), EVO

only increased protein expressions of TRAF2, ASK1, p-JNK, caspase-12, -9, -3, and Bax, and decreased Bcl-2 protein level. However, EVO treatment did not reverse 4-PBA-induced reduction in the expression levels of TRAF2, ASK1, p-JNK, caspase-12, -9, -3, and Bax or the increased expression of level of Bcl-2 compared with the 4-PBA pretreatment group (Figure 6(e)). Analogously, the increased *Traf2*, *Map3k5*, *Mapk9*, *Bax*, and diminished *Bcl-2* mRNA levels induced by EVO were not significant after 4-PBA pretreatment. Compared with the EVO only treatment group, the ratio of Bax/Bcl2 is also no longer different from the no treatment group following 4-PBA pretreatment. Additionally, there was no change in these gene mRNA levels or Bax/Bcl-2 ratio after EVO and 4-PBA intervention compared to the no-treatment group (Figure 6(f) and (g)). These results demonstrated that apoptosis in A549 and LLC cells was associated with ERS response.

Discussion

In the present study, we first established an LLC tumor-bearing model, which was treated with low-dose EVO (5 mg/kg) and high-dose EVO (10 mg/kg), to evaluate the efficacy of EVO as a potent anti-cancer candidate. As expected, our results showed that EVO significantly decreased tumor weight and volume. H&E staining also indicated that EVO treatment reduced the number of tumor cells and nucleo-plasmic ratio. Immunostaining indicated that EVO treatment markedly decreased the expression of Ki-67. We used CDDP treatment as a positive control, and this treatment had better effects in reducing tumor volume and increasing inhibition of Ki-67 expression compared with low-dose and high-dose EVO treatment. Additionally, there were no significant differences regarding tumor weight and tumor growth inhibition rate between CDDP and high-dose EVO treated mice. However, while it was more effective in some ways, CDDP causes drug resistance during the therapy and can induce life-threatening side effects such as cardiotoxicity, nephrotoxicity, and hepatotoxicity.

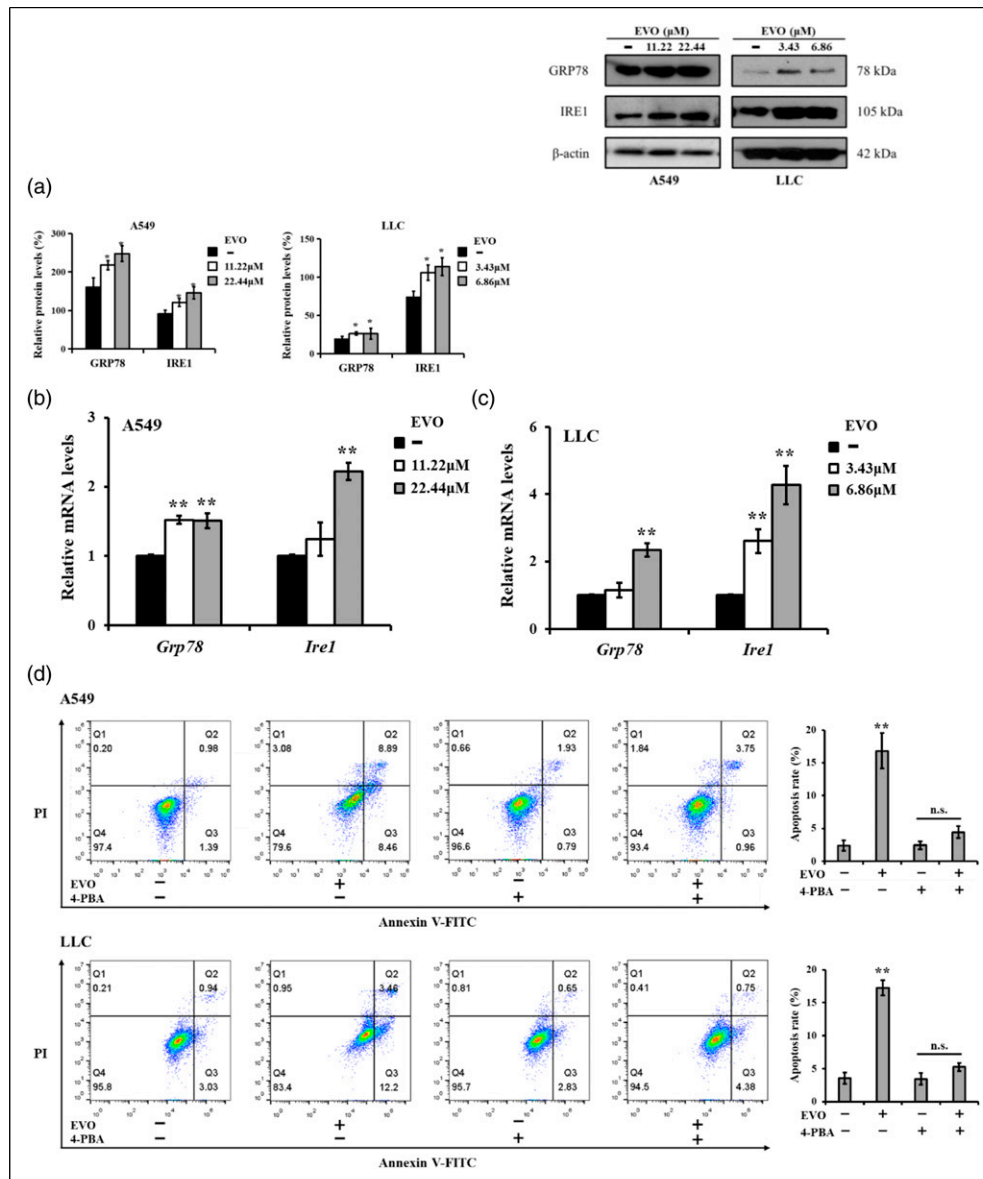


Figure 6. The effects of EVO on apoptosis were abolished after 4-PBA treatment. **(a)** EVO promoted the protein expressions of GRP78 and IRE1 in A549 and LLC cells. β -actin was used to confirm equal protein loading. **(b, c)** EVO raised the mRNA levels of *Grp78* and *Ire1*. A549 cells were treated with 11.22 μ M or 22.44 μ M EVO for 24h, while LLC cells were exposed to 3.43 or 6.86 μ M EVO for 48h. **(d)** EVO-induced apoptosis was observed by flow cytometry and indicated the apoptotic rate increased after EVO treatment. Data are expressed as mean \pm SD of at least three independent experiments. **(e)** The activation of apoptosis-related proteins by EVO were suppressed after 4-PBA intervention. β -actin was used to confirm equal protein loading. **(f, g)** EVO-induced increases in mRNA levels for *Traf2*, *Map3k5*, *Mapk9*, *Bax*, and the decrease in mRNA level for *Bcl2* were inhibited after 4-PBA pretreatment in A549 (f) and LLC (g) cells. Data are expressed as means \pm SD. A549 cells were treated with 22.44 μ M EVO for 24h while LLC cells were treated with 6.86 μ M EVO for 48h. *: $p < 0.05$ compared with EVO (-) group; **: $p < 0.01$ compared with EVO (-) group. Abbreviations: c-c12/t-c12: cleaved caspase-12/total caspase-12; c-c9/t-c9: cleaved caspase-9/total caspase-9; c-c3/t-c3: cleaved caspase-3/total caspase-3; n.s.: no significance.

Likewise, our results also showed increased of hepatic function factors (ALT and AST, [Supplementary Table S1](#)), renal function factors (Scr and BUN, [Supplementary Table S2](#)), and cardiac function factor (CK, [Supplementary Table S3](#)) in serum of LLC tumor-bearing mouse model after

CDDP treatment, whereas EVO treatment did not affect the hepatic, renal, and cardiac function factors in serum of LLC tumor-bearing mouse model. Despite our findings, which show that EVO is inferior to CDDP on several measures, the minimal difference between the two therapeutic test groups

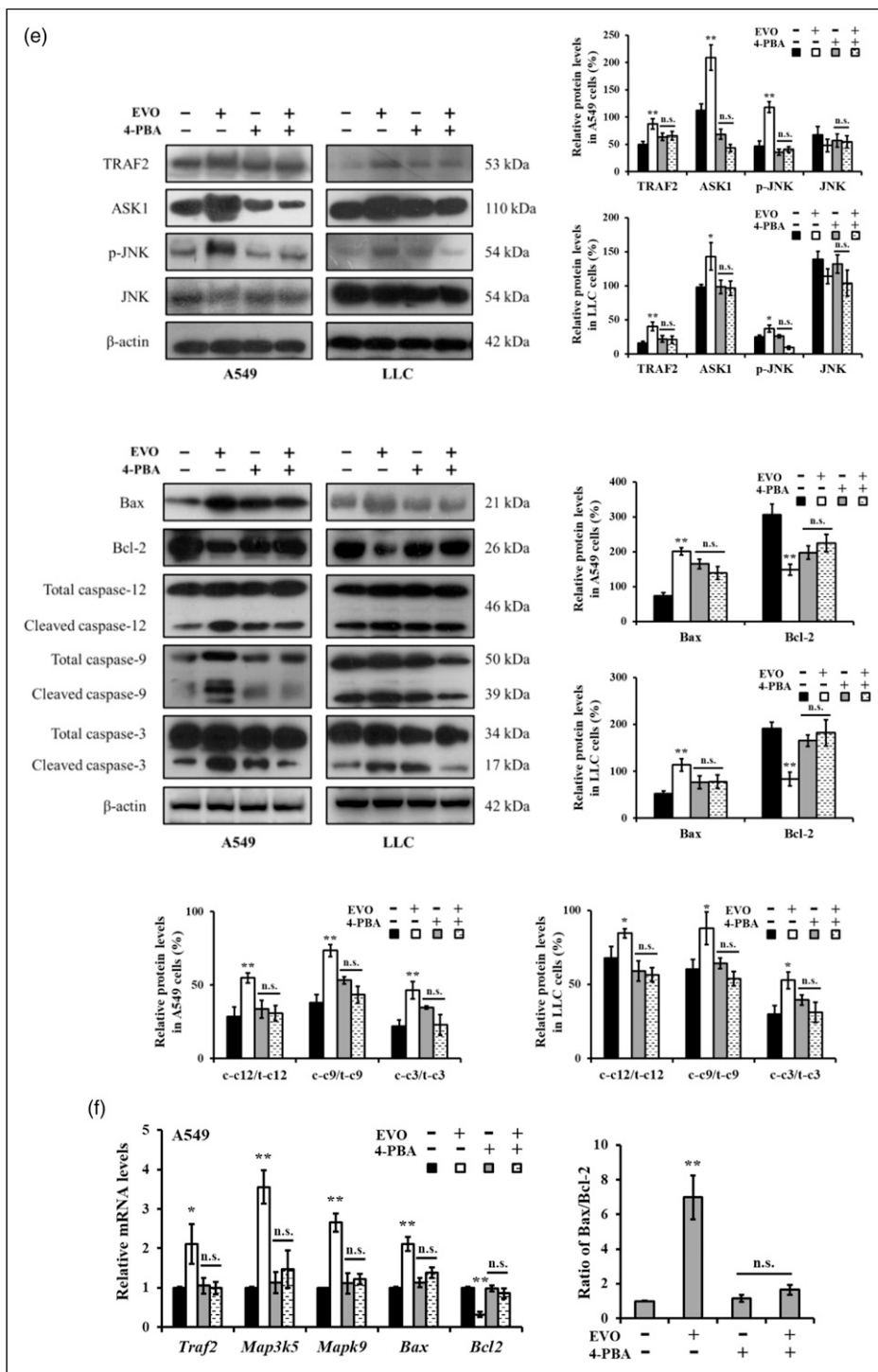


Figure 6. Continued.

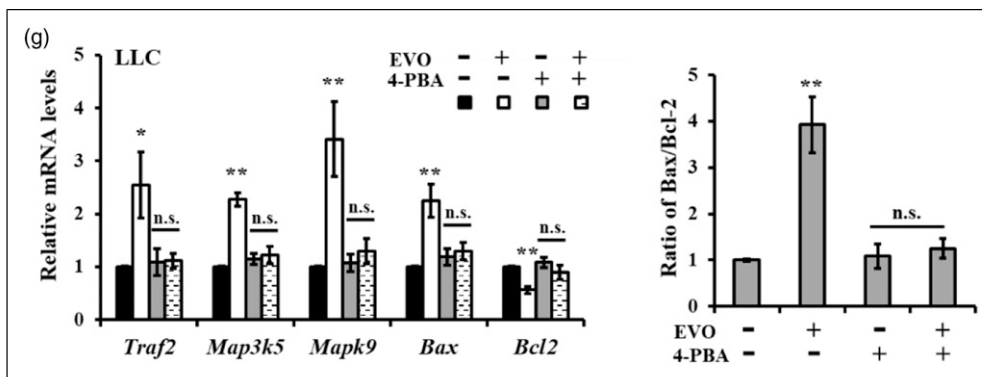


Figure 6. Continued.

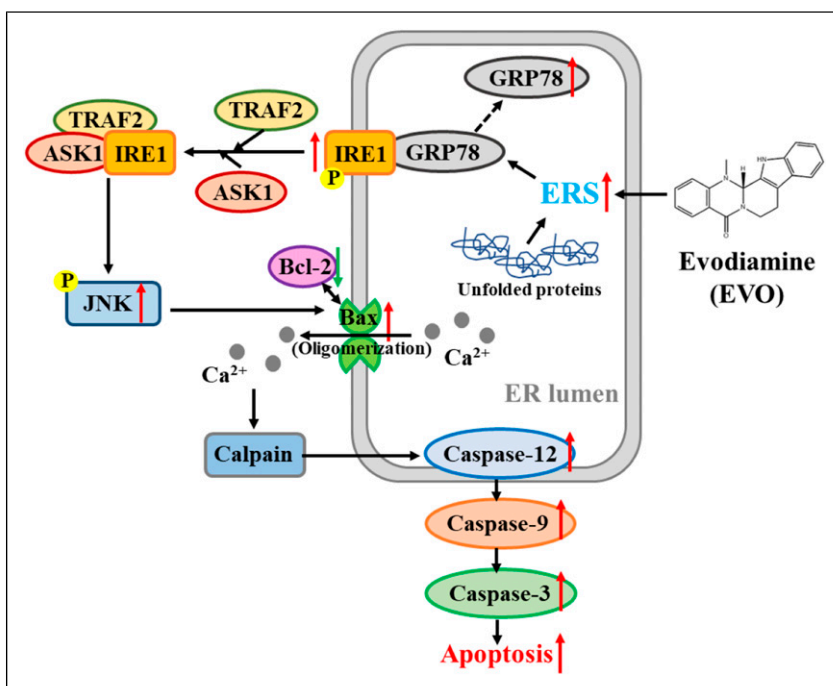


Figure 7. Graphical abstract of this study.

in other measures and the risks of using CDDP suggest that EVO may be an alternative treatment for NSCLC.

Cell apoptosis rates observed using TUNEL analysis and flow cytometry indicated that EVO elevated the apoptotic rates of A549 and LLC cells. Our results also revealed evidence both in vivo and in vitro of EVO-enhanced apoptosis from increased levels of Bax, caspases-12, -9, -3 and from the inhibition of Bcl-2. Apoptosis plays a key role in removing cancer cells, and caspase is one of the most important protease enzyme families which initiates and implements apoptosis.³² The caspase family is roughly separated into two groups: initiator caspases (caspase-12 and caspase-9) and effector caspases (caspase-3).³³ Initiator caspases undergo automatic activation in response to apoptotic

stimuli. In turn, active initiator caspases process precursors of the effector caspases to dismantle cellular structures.³⁴ In addition, the balance between pro-apoptotic proteins (Bax) and anti-apoptotic proteins (Bcl-2) in the Bcl-2 family is essential for effective apoptosis, and Bax binding to Bcl-2 will be inactivated without stimulation.³⁵⁻³⁷

Additional analyses demonstrated that EVO up-regulated the expression of ERS-associated proteins including GRP78, IRE1, TRAF2, ASK1, and p-JNK in vivo and in vitro. IRE1, an ER-resident trans-membrane protein, plays an essential role in the normal function of ER and UPR signaling pathways. Under physiological conditions, IRE1 is inactivated through binding to GRP78 (also known as Binding immunoglobulin heavy chain protein, Bip).³⁸

When the accumulation of unfolded proteins in the ER is excessive or prolonged, UPR initiates the apoptotic response.³⁹ After the disintegration of GRP78, IRE1 undergoes oligomerization and autophosphorylation in its kinase domain and becomes activated in response to ERS. Subsequently, activated IRE1, with kinase activity, binds TRAF2, recruiting ASK1 into IRE1/TRAF2/ASK1 complex formation and communicating the presence of ERS by activating JNK, a major mediator of apoptosis.^{40,41} The activation of ER-resident caspase-12 also depends on the recruitment of TRAF2 to IRE1.⁴² Additionally, recent data strongly suggest that Bax may be activated and Bcl-2 may be inhibited by the phosphorylation of JNK because Bax cannot activate in JNK-deficient fibroblasts following exposure to environmental stress.^{43,44} Moreover, the oligomerization of Bax, localized in the ER membrane, results in Ca²⁺ efflux from the ER lumen and activation of cytosolic calpain.⁴⁵ Calpain subsequently activates caspase-12, which is located on the cytoplasmic side of the ER membrane.⁴⁶ In turn, activated caspase-12 sets off the caspase cascade by cleavage and activation of caspase-9 and caspase-3 and results in cellular apoptosis.⁴¹ Notably, the activation of caspase-12 is induced by ERS but apparently not by death receptor-mediated or mitochondria-targeted apoptotic signals.⁴⁷ Thus, apoptosis could be triggered through ERS, and in our study, the ERS inhibitor 4-PBA was used to validate that EVO induced apoptosis via ERS. Results showed that EVO had no effect upon apoptosis-associated proteins or apoptotic rate when ERS was blocked by 4-PBA. These results indicate that EVO-induced cell apoptosis is associated with ERS (Figure 7).

Notably, there are some limitations in this study. First, we did not calculate and justify of the sample size in this study, and our future study will use statistic method to enhance the scientific rigor. Second, we did not observe the morphological changes on ER and our future study should be carried out to observe the morphological changes of subcellular structure in NSCLC cells after EVO treatment. Third, although our current results indicated that EVO treatment did not affect the hepatic, renal, and cardiac function factors in serum of LLC tumor-bearing mouse model, the detail toxicity of EVO in vivo should be studied after the development of EVO related-preparations. The in vivo toxicity of EVO could be the future research direction. Fourth, humanized tumor cell line-related tumor-bearing mouse model (e.g., A549 lung tumor bearing mouse model) should be used in future study to verify the anti-tumor effect of EVO.

Conclusions

Taken together, our study demonstrates EVO-induced apoptosis and ERS in LLC tumor-bearing mice and in NSCLC A549 and LLC cells. Notably, EVO-induced cell apoptosis, at least in part, occurs via the ERS-related

signaling pathway. These results support the potential that EVO could be an effective treatment for human NSCLC

Abbreviations

ASK1	apoptotic signal-regulating kinase 1
Bax	B-cell lymphoma-2 associated X protein
Bcl-2	B-cell lymphoma-2
Bip	binding immunoglobulin heavy chain protein; caspase, cysteinyl aspartate specific proteinase
CDDP	cisplatin
DAB	3,30-diaminobenzidine
DMEM	Dulbecco's modified eagle medium
DMSO	dimethyl sulfoxide
ERS	endoplasmic reticulum stress
ER	endoplasmic reticulum
EVO	evodiamine
FBS	fetal bovine serum
FITC	V-fluorescein isothiocyanate
GRP78	glucose-regulated protein 78
H&E	hematoxylin and eosin
IOD	integrated optical density
IRE1	inositol-requiring enzyme 1
JNK	c-JUN amino-terminal kinase
LLC	Lewis lung carcinoma
Map3k5	mitogen-activated protein kinase kinase kinase 5
MOD	mean optical density
MTT	[3-(4,5-dimethylthiazol-2-yl)2,5-diphenyltetrazolium bromide]
NSCLC	non-small cell lung carcinoma
PBS	phosphate-buffered saline
PI	propidium iodide
PS	penicillin/streptomycin
RPMI	Roswell park memorial institute
SDS-PAGE	sodium dodecyl sulfate-polyacrylamide gel electrophoresis
TBST	tween-tris-buffered saline
TRAF2	tumor necrosis factor receptor associated factor 2
TUNEL	terminal deoxynucleotidyl transferase-mediated dUTP nick end-labeling
UPR	unfolded protein response
4-PBA	4-phenylbutyric acid.

Author contributions

Yuting Li and Huantian Cui designed the project. Yuting Li, Yuming Wang, Lulu Jin, Lu Yang, and Xiaoqun Wang performed the experiments. Yuting Li, Yuming Wang, and Huantian Cui analyzed the data. Hongwu Wang, Fang Zheng, Yuting Li, Yingjie Jia, Jinli Zhu, and Xiaojiang Li supervised the experiments.

Yuting Li and Huantian Cui wrote and edited the manuscript. All authors reviewed the manuscript.

Declaration of Conflicting Interests

The author(s) declared no potential conflicts of interest with respect to the research, authorship, and/or publication of this article.

Funding

The author(s) disclosed receipt of the following financial support for the research, authorship, and/or publication of this article: This study is supported by National Natural Science Foundation of China (81904151).

Ethics approval

Ethical approval for this study was obtained from The Animal Experiment Ethics Committee of Tianjin University of Traditional Chinese Medicine (Registration No.: SYXK2019-0108).

Informed consent

Written informed consent was obtained from all subjects before the study.

Trial registration

The Animal Experiment Ethics Committee of Tianjin University of Traditional Chinese Medicine (Registration No.: SYXK2019-0108).

Data availability statement

All data were generated in-house, and no paper mill was used. All authors agree to be accountable for all aspects of work ensuring integrity and accuracy.

ORCID iD

Huantian Cui  <https://orcid.org/0000-0002-0820-5436>

Supplemental material

Supplemental material for this article is available online.

References

- International Agency for Research on Cancer (IARC). Available from <https://www.iarc.fr/faq/latest-global-cancer-data-2020-qa/>.
- Feng X, Yang S, Zhou S, et al. (2020) Long non-coding RNA DDX11-AS1 promotes non-small cell lung cancer development via regulating PI3K/AKT signalling. *Clin Exp Pharmacol Physiol* 47: 1622–1631.
- Pttgen C, Eberhardt W, Stamatidis G, et al. (2017) Definitive radiochemotherapy versus surgery within multimodality treatment in stage III non-small cell lung cancer (NSCLC) - a cumulative meta-analysis of the randomized evidence. *Oncotarget* 8: 41670–41678.
- Kang DH, Kim JO, Jung SS, et al. (2019) Efficacy of vinorelbine monotherapy as third- or further-line therapy in patients with advanced non-small-cell lung cancer. *Oncology* 97: 356–364.
- Oakes SA (2020) Endoplasmic reticulum stress signaling in cancer cells - sciencedirect. *Am J Pathol* 190: 934–946.
- Jaud M, Philippe C, Bella DD, et al. (2020) Translational regulations in response to endoplasmic reticulum stress in cancers. *Cells* 9: 540.
- Li XH, Wang YR, Wang H, et al. (2015) Endoplasmic reticulum stress is the crossroads of autophagy, inflammation, and apoptosis signaling pathways and participates in liver fibrosis. *Inflamm Res* 64: 1–7.
- Sharma S, Chaudhary P, Sandhir R, et al. (2021) Heat-induced endoplasmic reticulum stress in soleus and gastrocnemius muscles and differential response to UPR pathway in rats. *Cell Stress Chaperone* 26: 323–339.
- Chai Y, Zhu K, Li C, et al. (2020) Dexmedetomidine alleviates cisplatin induced acute kidney injury by attenuating endoplasmic reticulum stress induced apoptosis via the α 2AR/PI3K/AKT pathway. *Mol Med Rep* 21: 1597–1605.
- Kim C and Kim B (2018) Anti-cancer natural products and their bioactive compounds inducing ER stress-mediated apoptosis: a review. *Nutrients* 10: 1021.
- Han M, Han ZW, Gao H, et al. (2019) Hispidulin induces ERS-mediated apoptosis in human hepatocellular carcinoma cells in vitro and in vivo by activating AMPK signaling pathway. *Acta Pharmacol Sin* 40: 666–676.
- Liu Z, Sun Y, Ren L, et al. (2013) Evaluation of a curcumin analog as an anti-cancer agent inducing ERS-mediated apoptosis in non-small cell lung cancer cells. *BMC Cancer* 13: 494.
- Ren NN, Yang YY, Pan C, et al. (2018) A study on the effect of evodiamine on anti-oxidation and anti-inflammatory in rats with atherosclerosis. *J Guiyang Uni Chin Med* 40: 21–26.
- Kobayashi Y (2003) The nociceptive and anti-nociceptive effects of evodiamine from fruits of *Evodia rutaecarpa* in mice. *Planta Medica* 69: 425–428.
- Kobayashi Y, Nakano Y, Kizaki M, et al. (2001) Capsaicin-like anti-obese activities of evodiamine from fruits of *Evodia rutaecarpa*, a vanilloid receptor agonist. *Planta Med* 67: 628–633.
- Zhang ZX, Jiang ML, Wang XH, et al. (2014) Progress on pharmacological effect of evodiamine. *Prog Mod Biomed* 14: 4189–4191+4195.
- Jiang JL and Hu CP (2009) Evodiamine: a novel anti-cancer alkaloid from *evodia rutaecarpa*. *Molecules* 14: 1852–1859.
- Jiang ZB, Huang JM, Xie YJ, et al. (2020) Evodiamine suppresses non-small cell lung cancer by elevating CD8+ T cells and downregulating the MUC1-C/PD-L1 axis. *J Exp Clin Cancer Res* 39: 249.
- Li YL, Pan YN, Wu WJ, et al. (2016) Evodiamine induces apoptosis and enhances apoptotic effects of erlotinib in wild-

- type EGFR NSCLC cells via S6K1-mediated Mcl-1 inhibition. *Med Oncol* 33: 16–19.
20. Tu YJ, Fan X, Yang X, et al. (2013) Evodiamine activates autophagy as a cytoprotective response in murine Lewis lung carcinoma cells. *Oncol Rep* 29: 481–490.
 21. Fang C, Zhang J, Qi D, et al. (2014) Evodiamine induces G2/M arrest and apoptosis via mitochondrial and endoplasmic reticulum pathways in H446 and H1688 human small-cell lung cancer cells. *PLoS One* 9(12): e115204.
 22. Huh JE, Baek YH, Lee MH, et al. (2010) Bee venom inhibits tumor angiogenesis and metastasis by inhibiting tyrosine phosphorylation of VEGFR-2 in LLC-tumor-bearing mice. *Cancer Lett* 292: 98–110.
 23. Chen MF, Yang CM, Su CM, et al. (2011) Inhibitory effect of vitamin C in combination with vitamin K3 on tumor growth and metastasis of Lewis lung carcinoma xenografted in C57BL/6 mice. *Nutr Cancer* 63: 1036–1043.
 24. Zhu LQ, Zhang L, Zhang J, et al. (2021) Evodiamine inhibits high-fat diet-induced colitis-associated cancer in mice through regulating the gut microbiota. *J Integr Med* 19: 56–65.
 25. Zhang J, Zhang FH and Yang SJ (2017) Anticancer effects of Xi Huang Capsule on breast cancer in vivo. *Tradit Med Res* 2: 33–40.
 26. Cheng YC, Hueng DY, Huang HY, et al. (2016) Magnolol and honokiol exert a synergistic anti-tumor effect through autophagy and apoptosis in human glioblastomas. *Oncotarget* 7: 29116–29130.
 27. Xu XF, Cheng RB, Zhang XJ, et al. (2019) Total saponins in *Rubus parvifolius* L. induce lymphoma cells apoptosis through upregulated Bax/Fas and downregulated Bcl-2 in vivo and in vitro. *Tradit Med Res* 4: 99–108.
 28. Cui H, Cai Y, Wang L, et al. (2018) Berberine regulates treg/Th17 balance to treat ulcerative colitis through modulating the gut microbiota in the colon. *Front Pharmacol* 9: 571.
 29. Livak KJ and Schmittgen TD (2020) Analysis of relative gene expression data using real-time quantitative PCR and the 2^{-ΔΔC_T} method. *Methods* 25: 402–408.
 30. Guo G, Meng Y, Tan W, et al. (2015) Induction of apoptosis coupled to endoplasmic reticulum stress through regulation of CHOP and JNK in bone marrow mesenchymal stem cells from patients with systemic lupus erythematosus. *J Immunol Res* 2015: 183738.
 31. Zeng T, Peng LF, Chao HC, et al. (2015) IRE1α-TRAF2-ASK1 complex-mediated endoplasmic reticulum stress and mitochondrial dysfunction contribute to CXC195-induced apoptosis in human bladder carcinoma T24 cells. *Biochem Biophys Res Commun* 460: 530–536.
 32. Li J, Dong L, Zhu D, et al. (2020) An effector caspase Sp-caspase first identified in mud crab *Scylla paramamosain* exhibiting immune response and cell apoptosis. *Fish Shellfish Immunol* 103: 442–453.
 33. Szegezdi E, Fitzgerald U and Samali A (2003) Caspase-12 and ER-stress-mediated apoptosis: the story so far. *Ann N Y Acad Sci* 1010: 186–194.
 34. Grinshpon RD, Shrestha S, Titus-McQuillan J, et al. (2019) Resurrection of ancestral effector caspases identifies novel networks for evolution of substrate specificity. *Biochem J* 476: 3475–3492.
 35. Pihán P, Carreras-Sureda A and Hetz C (2017) BCL-2 family: integrating stress responses at the ER to control cell demise. *Cell Death Differ* 24: 1478–1487.
 36. Hetz CA (2007) ER stress signaling and the BCL-2 family of proteins: from adaptation to irreversible cellular damage. *Antioxid Redox Signal* 9: 2345–2356.
 37. Xia LM, Cui LL, Jiang YL, et al. (2017) Research on xijiao dihuang decoction suppressing platelet apoptosis in immune-mediated aplastic anemia based on mitochondrial mediated pathway. *Tradit Med Res* 2: 27–32.
 38. Dauer P, Sharma NS, Gupta VK, et al. (2019) ERS sensor, glucose regulatory protein 78 (GRP78) regulates redox status in pancreatic cancer thereby maintaining "stemness". *Cell Death Dis* 10: 132.
 39. Lin H, Peng Y, Li J, et al. (2021) Reactive Oxygen Species Regulate Endoplasmic Reticulum Stress and ER-Mitochondrial Ca²⁺ Crosstalk to Promote Programmed Necrosis of Rat Nucleus Pulposus Cells under Compression. *Oxid Med Cell Longev* 2021: 1–20.
 40. Mhaidat N M, Thorne R, Zhang X D, et al. (2008) Involvement of endoplasmic reticulum stress in Docetaxel-induced JNK-dependent apoptosis of human melanoma. *Apoptosis* 13: 1505–1512.
 41. Hiss DC and Gabriels GA (2009) Implications of endoplasmic reticulum stress, the unfolded protein response and apoptosis for molecular cancer therapy. Part II: targeting cell cycle events, caspases, NF-κB and the proteasome. *Expert Opin Drug Discov* 4: 907–921.
 42. Tong Q, Wu L, Jiang T, et al. (2016) Inhibition of endoplasmic reticulum stress-activated IRE1α-TRAF2-caspase-12 apoptotic pathway is involved in the neuroprotective effects of telmisartan in the rotenone rat model of Parkinson's disease. *Eur J Pharmacol* 776: 106–115.
 43. Lei K, Nimmual A, Zong WX, et al. (2002) The Bax subfamily of Bcl2-related proteins is essential for apoptotic signal transduction by c-Jun NH(2)-terminal kinase. *Mol Cell Biol* 22: 4929–4942.
 44. Kim BJ, Ryu SW and Song BJ (2006) JNK- and p38 kinase-mediated phosphorylation of Bax leads to its activation and mitochondrial translocation and to apoptosis of human hepatoma HepG2 cells. *J Biol Chem* 281: 21256–21265.
 45. Nakano T, Watanabe H, Ozeki M, et al. (2006) Endoplasmic reticulum Ca²⁺ depletion induces endothelial cell apoptosis independently of caspase-12. *Cardiovasc Res* 69: 908–915.
 46. Martinez JA, Zhang Z, Svetlov SI, et al. (2010) Calpain and caspase processing of caspase-12 contribute to the ERS-induced cell death pathway in differentiated PC12 cells. *Apoptosis* 15: 1480–1493.
 47. Oyadomari S, Araki E and Mori M (2002) Endoplasmic reticulum stress-mediated apoptosis in pancreatic β-cells. *Apoptosis* 7: 335–345.